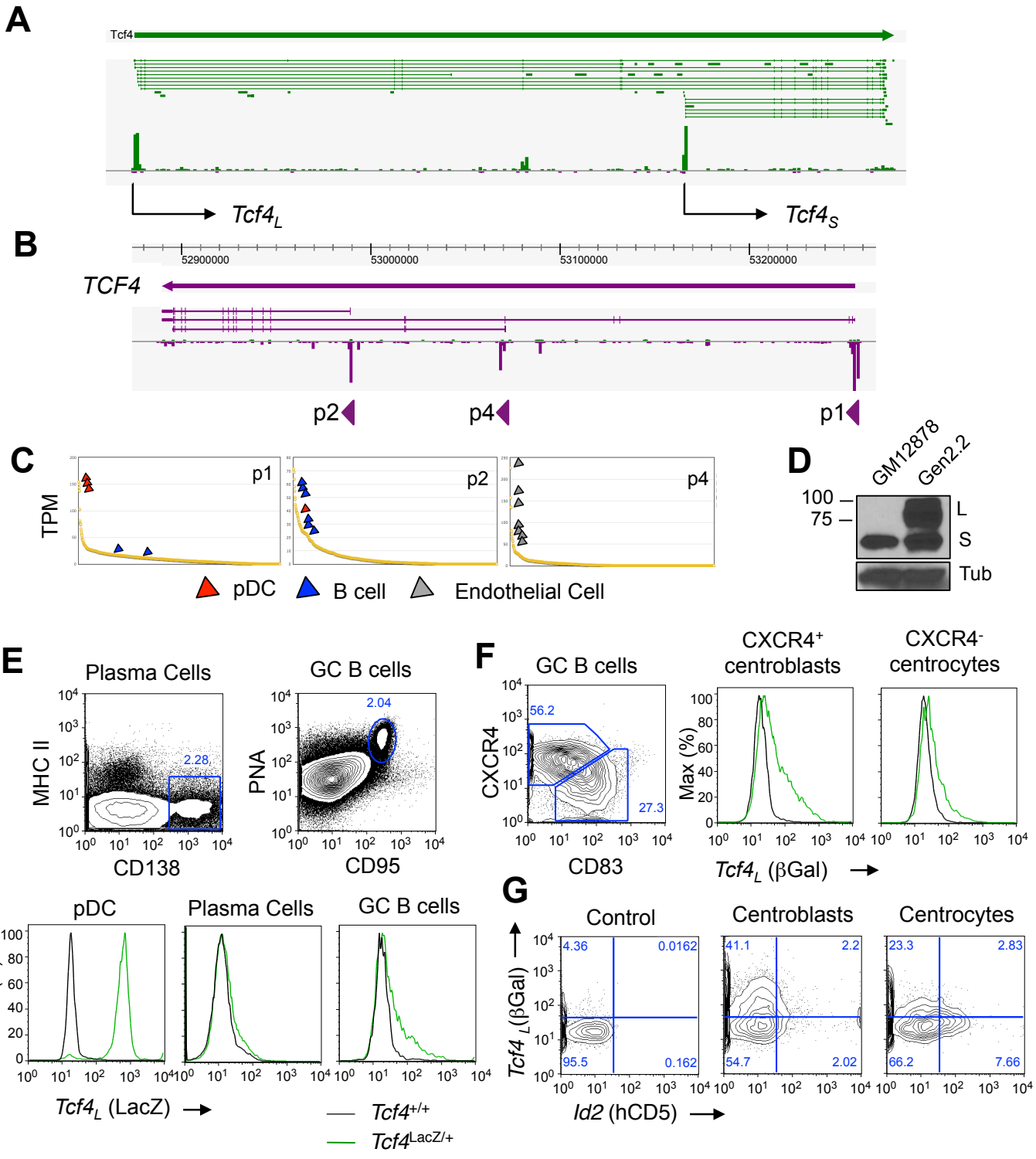
A
Tcf4
Tcf4L
Tcf4S
B
52900000
53000000
53100000
53200000
TCF4
p2
p4
p1
C
TPM
p1
p2
p4
pDC
B cell
Endothelial Cell
D
GM12878
Gen2.2
100
75
L
S
Tub
E
Plasma Cells
GC B cells
MHC II
CD138
2.28
PNA
CD95
2.04
pDC
Plasma Cells
GC B cells
Max (%)
Tcf4L (LacZ)
Tcf4+/+
Tcf4LacZ/+
F
GC B cells
CXCR4+ centroblasts
CXCR4- centrocytes
CXCR4
CD83
56.2
27.3
Max (%)
Tcf4L (βGal)
G
Control
Centroblasts
Centrocytes
Tcf4 L(βGal)
Id2 (hCD5)
4.36
0.0162
95.5
0.162
41.1
2.2
54.7
2.02
23.3
2.83
66.2
7.66

Figure S1, related to Fig. 1. Cell type-specific expression of *Tcf4* isoforms

(A) Transcriptional map of the murine *Tcf4* locus. Shown are major annotated transcripts and the 5' transcription sites in the FANTOM Atlas, in the sense (green) or antisense (purple) orientation relative to *Tcf4*. The two major transcription start sites corresponding to the long ($Tcf4_L$) and short ($Tcf4_S$) isoforms are indicated.

(B) Transcriptional map of the human *TCF4* locus, including major annotated transcripts and the 5' transcription sites in the FANTOM Atlas, in the sense (purple) or antisense (green) orientation relative to *TCF4*. The three major promoters corresponding to $TCF4_L$ (p1), $TCF4_S$ (p2) and a third isoform (p4) are indicated.

(C) Expression of the three promoters across cells and tissues in the FANTOM database. Samples corresponding to human primary pDCs, B cells and endothelial cells are indicated. TPM, transcripts per million reads.

(D) Western immunoblot analysis of TCF4 protein expression in the human B cell line GM12878 and pDC line Gen2.2. Tubulin was used as a loading control.

(E) The expression of $Tcf4_L$ in the germinal center (GC) B cells. Wild-type $Tcf4^{+/+}$ and heterozygous reporter $Tcf4^{LacZ/+}$ mice were immunized with sheep red blood cells (SRBC) and analyzed 14 days later. Shown are representative staining profiles of $B220^+$ B cells with $CD138^+$ plasma cells or PNA^+ $CD95^+$ GC B cells highlighted, and the expression of βGal in these gated populations. The expression in pDCs is shown for comparison.

(F) The expression of $Tcf4_L$ in germinal center (GC) subsets. Shown are GC B cells from SRBC-immunized reporter mice subdivided into $CXCR4^+$ $CD83^-$ centroblasts and $CXCR4^-$ $CD83^+$ centrocytes, and the expression of βGal in these gated populations.

(G) The expression of $Tcf4_L$ and *Id2* in the subsets of germinal center GC B cells gated as above in SRBC-immunized $Tcf4^{LacZ/+}$ $Id2^{hCD5/hCD5}$ mice.

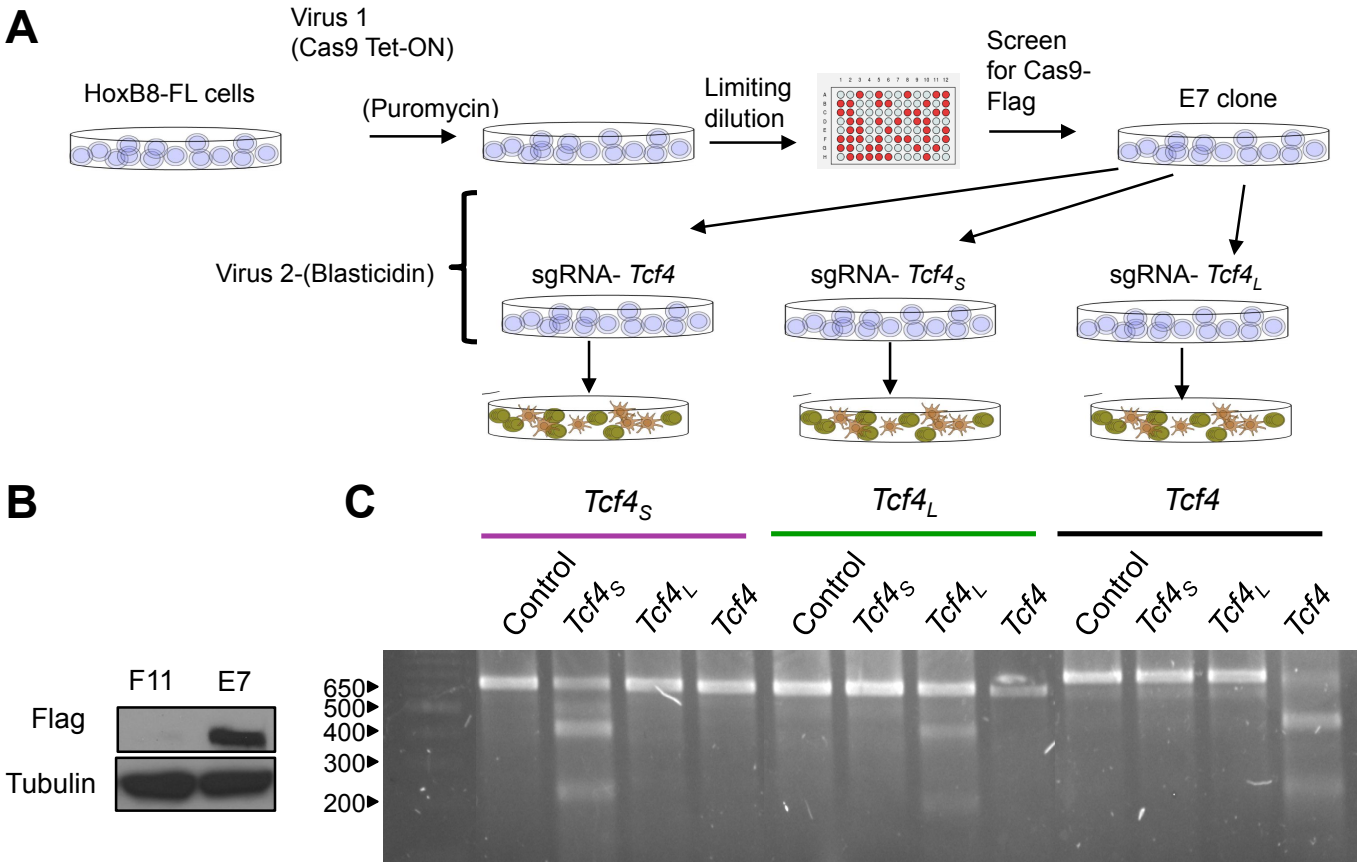

Figure S2, related to Fig 2. CRISPR/Cas9 targeting of *Tcf4* isoforms
(A) The strategy of targeting individual *Tcf4* isoforms by sgRNA and/or Cas9-expressing lentiviruses in the HoxB8-FL cells.
(B) Western immunoblot analysis of Flag-tagged Cas9 (anti-Flag Ab) in clones transduced with the Cas9 lentivirus. The Cas9-expressing clone E7 was used for subsequent targeting.
(C) Detection of genomic alterations in the targeted *Tcf4* isoforms. Genomic DNA was extracted from undifferentiated HoxB8-FL cells that were ttransduced with lentivirally expressed sgRNA for exons specific for $Tcf4_L$ or $Tcf4_S$ isoforms or a common *Tcf4* exon (color-coded above). Each DNA samples was assayed by the T7 cleavage assay for alterations in a control irrelevant genomic region or in exons specific for either or both isoforms. Note that genomic alterations (as evidenced by the reduction of the germline band and the appearance of additional bands) occur only in the exons targeted by each sgRNA. Also note that the assay underestimates the extent of genomic alteration because it fails to detect identical biallelic alterations.

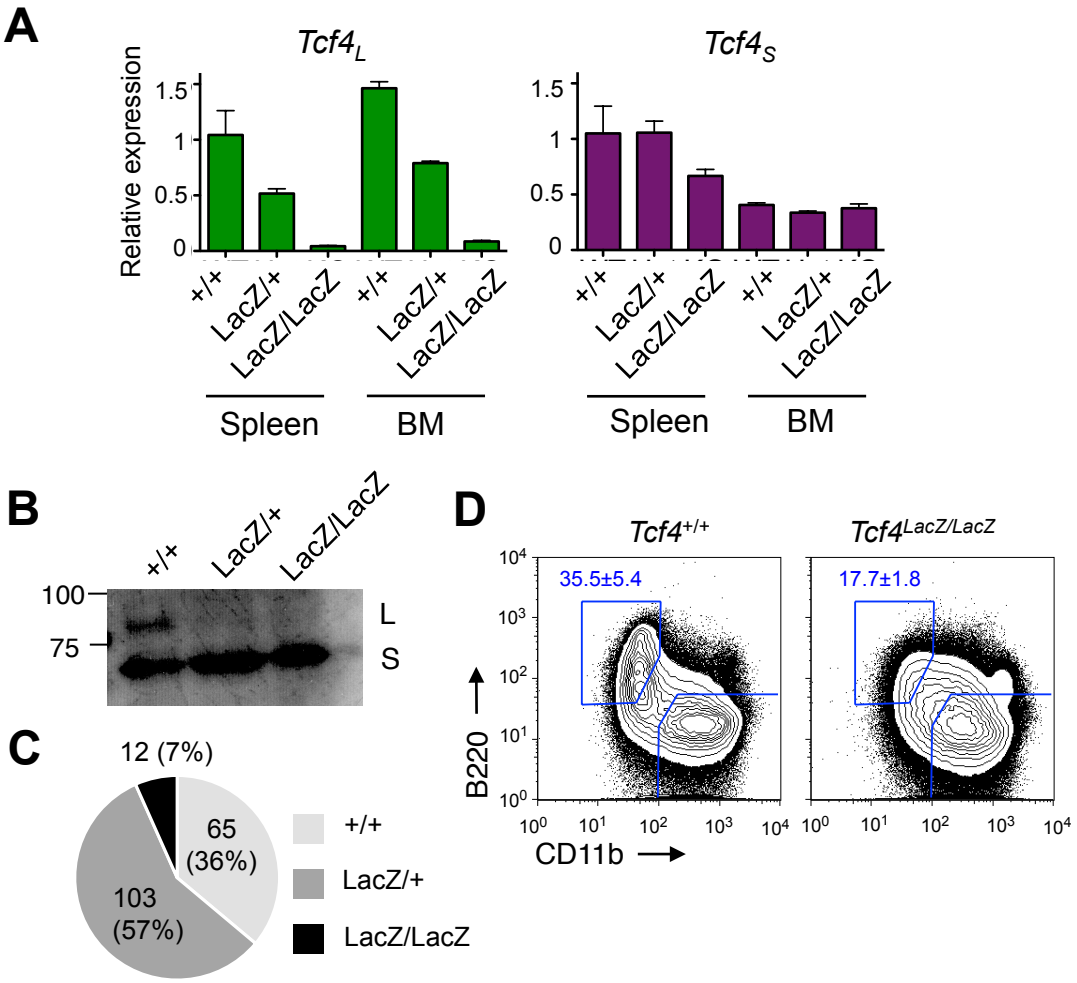

Figure S3, **related to Fig. 3. The *Tcf4*^{LacZ} allele specifically ablates the expression of TCF4$_L$**
(A) The expression of *Tcf4* isoform transcripts in *Tcf4*^{LacZ}-carrying animals. Total spleen and BM cells from littermate mice of indicated genotypes were analyzed by qRT-PCR for *Tcf4* isoforms. Data represent transcript levels of each isoform relative to the wild-type spleen sample (mean ± S.D. of triplicate PCR reactions).
(B) Western immunoblot analysis of TCF4 protein expression in total BM cells from mice of indicated genotypes.
(C) The distribution of genotypes at 2 weeks of age in the progeny of *Tcf4*$^{LacZ/+}$ intercross. Total number of animals from 26 litters is indicated for each genotype.
(D) pDC development in Flt3L-supplemented cultures of the BM from *Tcf4*$^{+/+}$ or *Tcf4*$^{LacZ/LacZ}$ mice. The fractions of B220$^+$ pDCs and CD11b$^+$ cDCs are indicated (mean ± range of 2 mice).

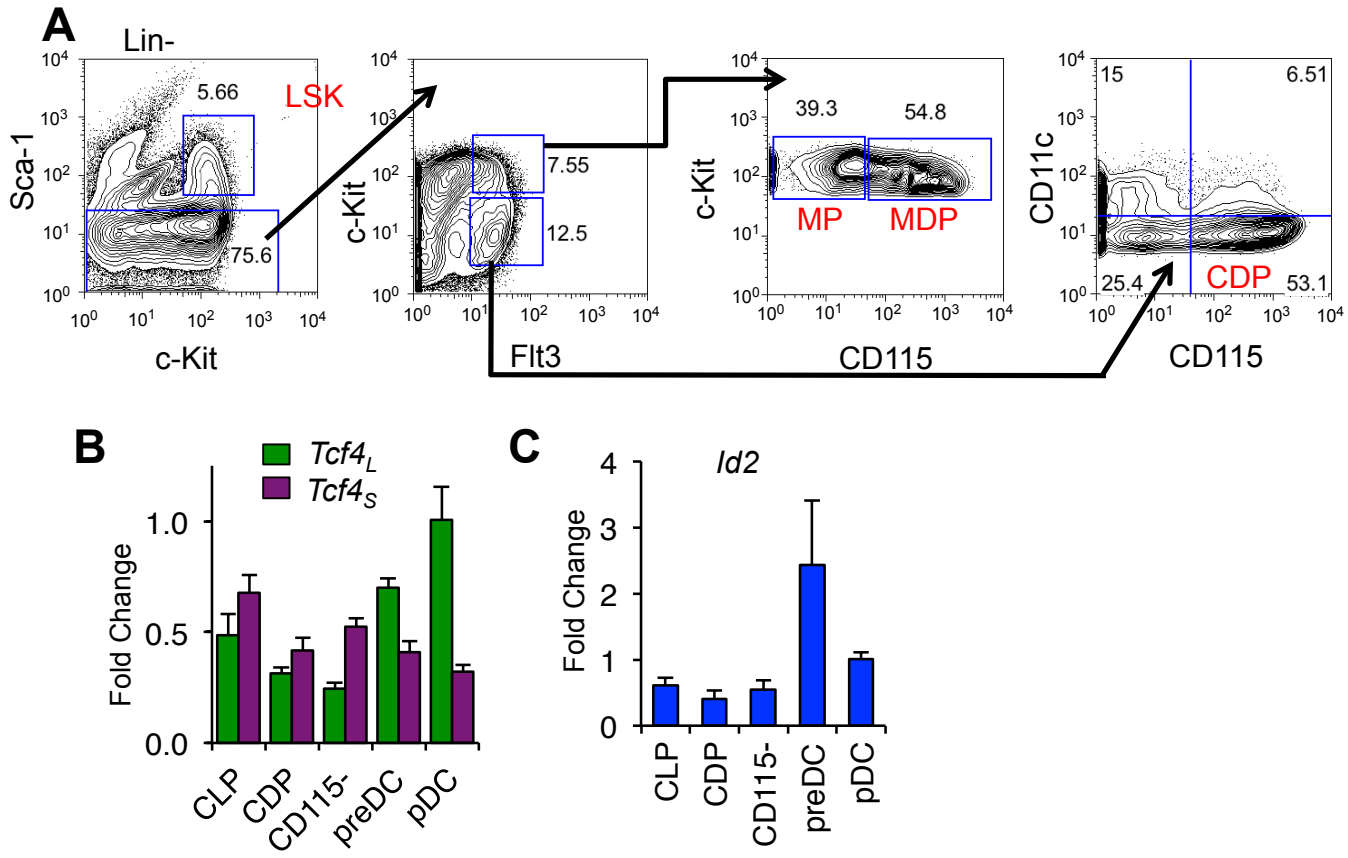

Figure S4, related to Fig. 4. The expression of *Tcf4* in hematopoietic progenitors.
(A) Gating strategy for progenitor staining. Lin^- BM cells from wild-type mice were gated as indicated to define the progenitor populations shown in Figure 4B.
(B) The expression of *Tcf4* isoform transcripts in sorted stem/progenitor populations from wild-type mice. The Lin^- BM populations including common lymphoid progenitors (CLP, $Flt3^+$ IL-$7R^+$ $CD11c^-$), CDP ($Flt3^+$ IL-$7R^-$ $CD11c^-$ $CD115^+$), $CD115^-$ CDP (Lin^- $Flt3^+$ IL-$7R^-$ $CD11c^-$ $CD115^-$), pre-DC (Lin^- $Flt3^+$ IL-$7R^-$ $CD11c^+$) were analyzed by qRT-PCR for TCF4 isoforms. Data represent transcript levels relative to $TCF4_L$ in pDCs (mean ± S.D. of triplicate PCR reactions).
(C) The expression of *Id2* in the stem/progenitor populations described above, as determined by qRT-PCR (mean ± S.D. of triplicate PCR reactions).

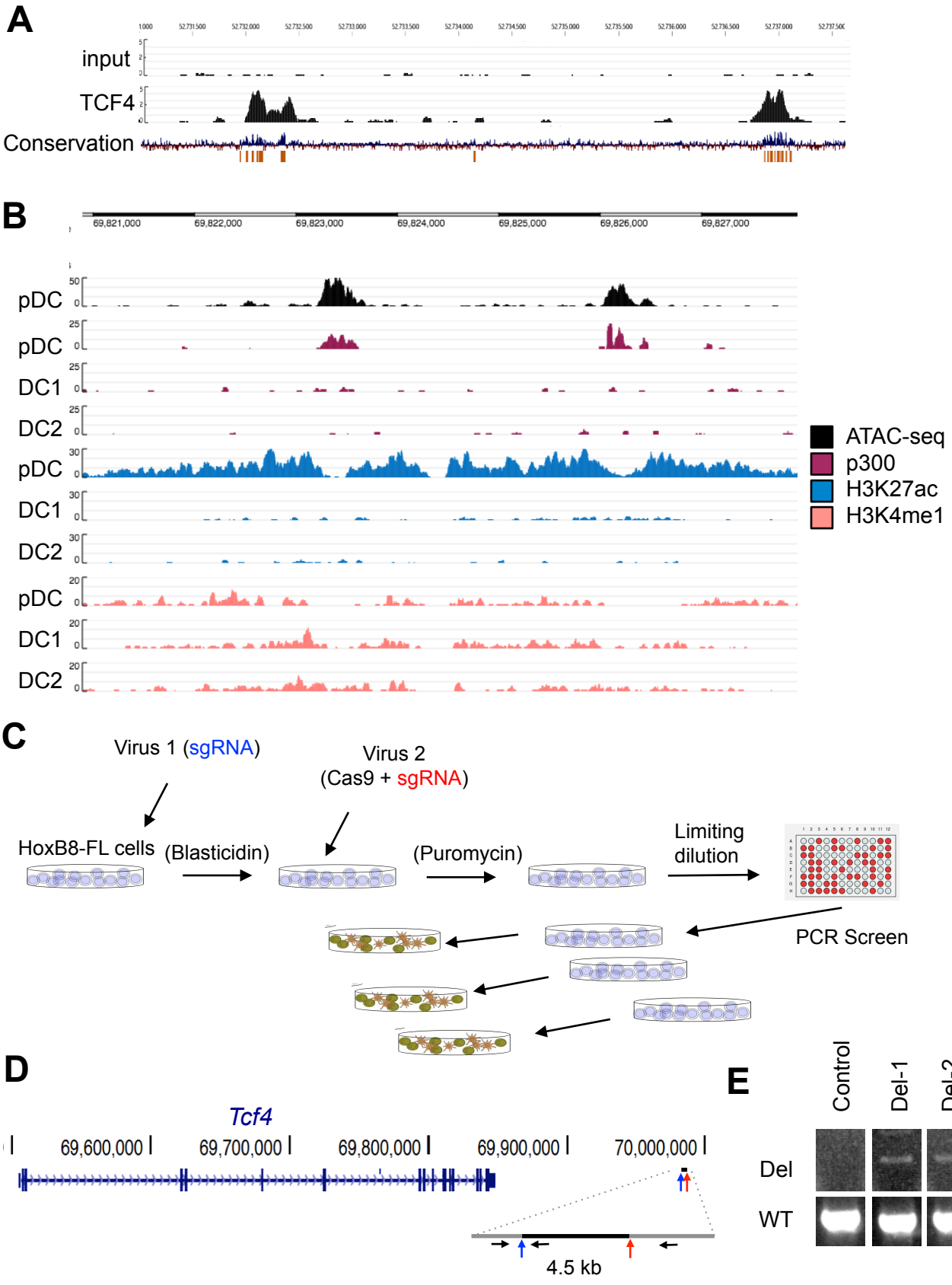
A
input
TCF4
Conservation
B
69,821,000
69,822,000
69,823,000
69,824,000
69,825,000
69,826,000
69,827,000
pDC
pDC
DC1
DC2
pDC
DC1
DC2
pDC
DC1
DC2
ATAC-seq
p300
H3K27ac
H3K4me1
C
Virus 1 (sgRNA)
Virus 2
(Cas9 + sgRNA)
HoxB8-FL cells
(Blasticidin)
(Puromycin)
Limiting
dilution
PCR Screen
D
Tcf4
69,600,000
69,700,000
69,800,000
69,900,000
70,000,000
4.5 kb
E
Control
Del-1
Del-2
Del
WT

Figure S5, related to Fig. 5. Characterization of the 3' regulatory element of *TCF4*.
(A) TCF4 ChIP-Seq analysis in human CAL-1 pDC cell line. Shown is TCF4 binding (data from (Ghosh et al., 2014)) and conservation in mammalian species (from the UCSC Genome Browser).
(B) ChIP-seq analysis of the 3' enhancer region for p300 binding, H3K27ac and H3K4me1 in BM-derived DC populations. Data are from (Grajales-Reyes et al., 2015).
(C) The strategy of targeting the 3' enhancer by sgRNA/CAS9-expressing lentiviruses in the HoxB8-FL cells.
(D) Schematic of the targeted region in the mouse *Tcf4* locus, showing sgRNAs (vertical arrows) and genotyping primers (horizontal arrows)
(E) Genomic PCR of the targeted clones, showing the products of the wild-type (WT) and deleted (Del) alleles.

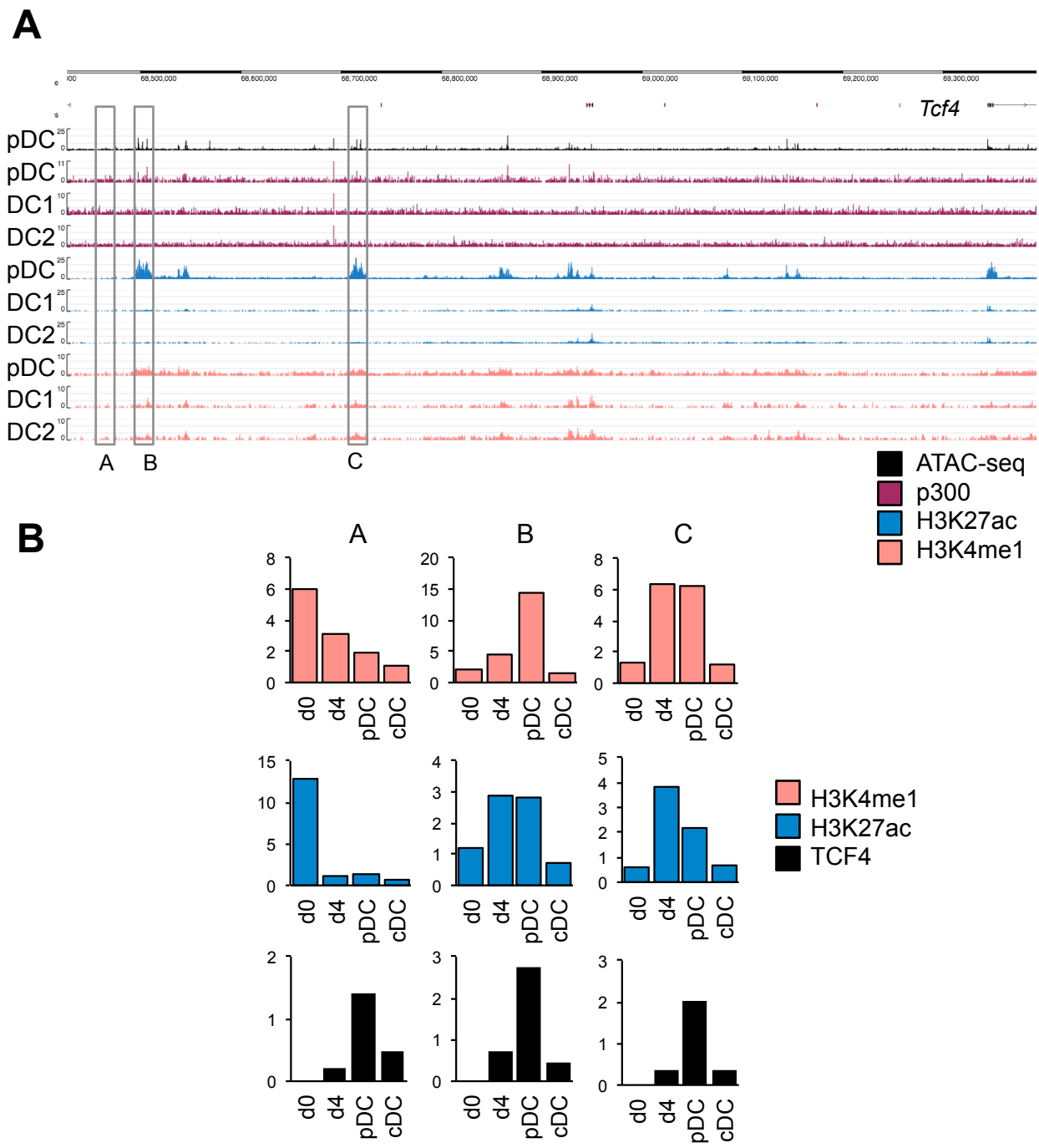

Figure S6, related to Fig 6. Characterization of the 5' regulatory elements of *Tcf4*.
(A) ATAC-Seq and p300, H3K27ac, and H3K4me1 ChIP-Seq analysis of the 5' region of the *Tcf4* locus, with the regions of interest indicated.
(B) ChIP analysis of histone modifications (H3K4me1 and H3K27ac) and of TCF4 binding to the indicated 5' regulatory regions in differentiating HoxB8-FL cells. Shown is fold enrichment of bound regions over a control region in undifferentiated (day 0), differentiating (day 4) and mature pDC and cDC on day 7.

Supplemental Methods

Genome data analysis. FANTOM consortium data were visualized using the ZENBU genome browser (Andersson et al., 2014; Forrest et al., 2014). ATAC-Seq data on primary murine hematopoietic cell types (HSC, MPP, CLP, B cells and NK cells) were from (Shih et al., 2016) and those on primary murine neurons were from (Mo et al., 2015). ATAC-Seq on primary pDC, DC1 and DC2 populations sorted from normal mouse spleens was done as described (Buenrostro et al., 2013) and will be described in detail elsewhere. ChIP-Seq on DC populations derived from Flt3L-supplemented BM cultures were from (Grajales-Reyes et al., 2015). All primary sequencing data were mapped to the mouse genome (version mm10) using the Bowtie2 (Langmead and Salzberg, 2012) software and visualized using the Biodalliance genome browser (Down et al., 2011).

Human cell lines. The human pDC cell line Gen2.2 was kindly provided by Drs. L. Chaperot and J. Plumas (EFS Rhone-Alpes Grenoble, France) and cultured as described (Chaperot et al., 2006). The human B cell lymphoblastoid line GM12878 was obtained from the Coriell Cell Repositories and cultured as suggested by the distributor.

PCR primers. The expression of the two *Tcf4* isoforms was detected with forward primers specific to each isoform, and a common reverse primer:
$TCF4_L$ F: 5'-CCAGGAACCCTTTCGCCCACCAAAC-3'
$TCF4_S$ F: 5'-ATCCCGGGCATGGGCGGCAACTC-3'
Common R: 5'-TGCTGGCTGCTGGCTTGGAGGAA-3'

Both primer sets showed similar amplification efficiency against the titrated amounts of template. The expression of *Id2* was detected with the primers:
F: 5'-GAGAACGACACCTGGGCAAGA-3'
R: 5'-CGTCAGCCTGCATCACCAGA-3'

For ChIP, immunoprecipitated genomic DNA was analyzed by qPCR for enrichment of enhancer regions using the primers:
3' Enhancer F 5'-CTCTCGGTGGGTTAGCACTT-3
3' Enhancer R 5'-CTTCTTTGAATCTGAGCAGTGTGG-3'
5' element (A) F 5'-CAAGGCGAGGGAAGCCG-3'
5' element (A) R 5'-GGAGGCCACCAAGAACCTAC-3'
5' element (B) F 5'-CCTGGTGAGGGATGTGGAAC-3'
5' element (B) R 5'-CGGACTTGTGTTCCGATGTTCA-3'
5' element (C) F 5'-CGGACTTTGTTCCGATGTTCA-3'
5' element (C) R 5'-CCAGCCGATGCTTGTCCTTC-3'
Control F 5'-AGATGAGTCCTGCAAAGGGC-3'
Control R 5'-GCTAACCTGCTAACCAGCCA-3'

Targeting of *Tcf4* isoforms. To express Cas9 in HoxB8-FL cells, we used pCW-Cas9 (Addgene #50661) (Wang et al., 2014) vector that contains a doxycycline-inducible Cas9 and confers puromycin resistance. VSV-G-pseudotyped lentiviral particles were produced using transient transfection in 293T cells. Undifferentiated HoxB8-FL cells were spinoculated with the Cas9 vector and batch selected with puromycin. The resulting population was cloned by limiting dilution and screened for the expression of FLAG-tagged Cas9 after doxycycline treatment by anti-Flag Western analysis. All clones showed some Cas9 expression without doxycycline, hence the inducibility feature was not used and all targetings were performed in the presence of doxycycline. Clone E7 with the highest expression of Cas9 was chosen and used for targeting. SgRNAs targeting either TCF4 isoforms or a common TCF4 exon were cloned into the pLX-sgRNA lentiviral vector (Addgene #50662) (Wang et al., 2014) that confers blasticidin resistance. SgRNA sequences were as follows:
Tcf4L: 5'-AGCCCGTCCAGGGTAAGTAT-3'
Tcf4S:5'-CGCATACACCATCCCGGGCA-3'
TCF4 common: 5'-GAGGGTCCGAGATATCAACG-3'

Undifferentiated HoxB8-FL clone E7 was spinoculated with the sgRNA-containing vectors and batch selected with blasticidin. The resulting batch populations were confirmed for correct targeting usin the T7E1 assay and Western blot, and used for pDC differentiation.

Targeting of the 3' enhancer. The enhancer element was targeted using sgRNA flanking the entire enhancer region:
5' sgRNA: 5'-ATTGGGAGTCTGACCAAATTC-3'
3' sgRNA: 5'-ATTAAAAGACTCGGGAGCGT-3'

The 5' sgRNA was cloned into the pLX-sgRNA lentiviral vector (Addgene #50662) (Wang et al., 2014) that confers blasticidin resistance. The 3' sgRNA was cloned into the LentiCRISPR v2 vector (Addgene #52961) (Sanjana et al., 2014) that also encodes Cas9 and confers puromycin resistance. VSV-G-pseudotyped lentiviral particles were produced from both vectors using transient transfection in 293T cells. Undifferentiated HoxB8-FL cells were spinoculated with the 5' sgRNA vector, batch-selected with blasticidin, spinoculated with the 3' sgRNA vector and batch-selected with puromycin. The resulting population was either analyzed in bulk or cloned by

seeding 0.3 cells/well in 96 well plates, and the resulting clones were screened by PCR for the wild-type and targeted alleles using genotyping primers
Forward: 5'-TCAATCTCAGACTGGGTAGGGAAT-3'
Reverse wild-type: 5'-ATCCCCCCTGGCTTTCTTTGCT-3'
Reverse targeted: 5'-GTGCATGCCTATTTGTTCGGG-3'.

T7 endonuclease I (T7E1) mismatch cleavage assay. Cells were lysed with DNazol Direct (Molecular Research Center, Inc) and ~50 ng of genomic DNA extract was used to PCR-amplify a 600-700 bp region containing the targeted site using Q5 Hot Start High-Fidelity 2X Master Mix (NEB). Primer pairs were designed to flank the target region with the sgRNA sequence being set offset from the center of the amplicon. Primer sequences used for amplification of genomic regions containing the targeted sites for long (*Tcf4*$_L$), short (*Tcf4*$_S$) or both (*Tcf4*) E2-2 isoforms were as follows: *Tcf4* forward 5'- TAAACCAACCCCAAGGTCAG -3' and reverse 5'-GCCTCAGTTCCCAGTGAGAG - 3'; *Tcf4*$_L$ forward 5'- GTCAGGAGCCACTGTCATCA -3'; and reverse 5'-CACCTGTGCTGGGCATATTA -3'; *Tcf4*$_S$ forward 5'- ACTTGAGCGTCTGACAGCAG -3' and reverse 5'-CTGCTCCTCCTTCCAATCAT -3'. Following amplification, PCR products were denatured and re-annealed in NEBuffer 2 (NEB) using a thermocycler to allow DNA heteroduplex formation. Hybridized PCR products were digested with T7 endonuclease I (NEB) at 37^{O}C for 15 minutes. The digestion was stopped by incubating with 1uL Proteinase K for 5 minutes at 37^{O}C and DNA fragments were separated by 3% agarose gel electrophoresis.

Supplemental References

Andersson, R., Gebhard, C., Miguel-Escalada, I., Hoof, I., Bornholdt, J., Boyd, M., Chen, Y., Zhao, X., Schmidl, C., Suzuki, T.*, et al.* (2014). An atlas of active enhancers across human cell types and tissues. Nature *507*, 455-461.

Buenrostro, J.D., Giresi, P.G., Zaba, L.C., Chang, H.Y., and Greenleaf, W.J. (2013). Transposition of native chromatin for fast and sensitive epigenomic profiling of open chromatin, DNA-binding proteins and nucleosome position. Nat Methods *10*, 1213-1218.

Chaperot, L., Blum, A., Manches, O., Lui, G., Angel, J., Molens, J.P., and Plumas, J. (2006). Virus or TLR agonists induce TRAIL-mediated cytotoxic activity of plasmacytoid dendritic cells. J Immunol *176*, 248-255.

Down, T.A., Piipari, M., and Hubbard, T.J. (2011). Dalliance: interactive genome viewing on the web. Bioinformatics *27*, 889-890.

Forrest, A.R., Kawaji, H., Rehli, M., Baillie, J.K., de Hoon, M.J., Haberle, V., Lassman, T., Kulakovskiy, I.V., Lizio, M., Itoh, M.*, et al.* (2014). A promoter-level mammalian expression atlas. Nature *507*, 462-470.

Ghosh, H.S., Ceribelli, M., Matos, I., Lazarovici, A., Bussemaker, H.J., Lasorella, A., Hiebert, S.W., Liu, K., Staudt, L.M., and Reizis, B. (2014). ETO family protein Mtg16 regulates the balance of dendritic cell subsets by repressing Id2. J Exp Med *211*, 1623-1635.

Grajales-Reyes, G.E., Iwata, A., Albring, J., Wu, X., Tussiwand, R., Kc, W., Kretzer, N.M., Briseno, C.G., Durai, V., Bagadia, P.*, et al.* (2015). Batf3 maintains autoactivation of Irf8 for commitment of a CD8alpha(+) conventional DC clonogenic progenitor. Nature immunology *16*, 708-717.

Langmead, B., and Salzberg, S.L. (2012). Fast gapped-read alignment with Bowtie 2. Nat Methods *9*, 357-359.

Mo, A., Mukamel, E.A., Davis, F.P., Luo, C., Henry, G.L., Picard, S., Urich, M.A., Nery, J.R., Sejnowski, T.J., Lister, R.*, et al.* (2015). Epigenomic Signatures of Neuronal Diversity in the Mammalian Brain. Neuron *86*, 1369-1384.

Sanjana, N.E., Shalem, O., and Zhang, F. (2014). Improved vectors and genome-wide libraries for CRISPR screening. Nat Methods *11*, 783-784.

Shih, H.Y., Sciume, G., Mikami, Y., Guo, L., Sun, H.W., Brooks, S.R., Urban, J.F., Jr., Davis, F.P., Kanno, Y., and O'Shea, J.J. (2016). Developmental Acquisition of Regulomes Underlies Innate Lymphoid Cell Functionality. Cell *165*, 1120-1133.

Wang, T., Wei, J.J., Sabatini, D.M., and Lander, E.S. (2014). Genetic screens in human cells using the CRISPR-Cas9 system. Science *343*, 80-84.